Quantum Information and Computation, Vol. 14, No. 3&4 (2014) 0255–0264


# DYNAMICS OF MULTI-QUBIT STATES IN NON-INERTIAL FRAMES FOR QUANTUM COMMUNICATION APPLICATIONS

ALAA SAGHEER
*Center for Artificial Intelligence and RObotics(CAIRO)*
*Department of Mathematics, Aswan University*
*Aswan, Sahari 81528, Egypt*
*alaa@cairo-aswu.edu.eg*

HALA HAMDOUN
*Center for Artificial Intelligence and RObotics(CAIRO)*
*Aswan University*
*Aswan, Sahari 81528, Egypt*
*hala@cairo-aswu.edu.eg*

Received December 9, 2012
Revised May 24, 2013

In this paper, some properties of multi-qubit states traveling in non-inertial frames are investigated, where we assume that all particles are accelerated. These properties are including fidelities, capacities and entanglement of the accelerated channels for three different states, namely, Greeberger-Horne-Zeilinger (GHZ) state, GHZ-like state and W-state. It is shown here that all these properties are decreased as the accelerations of the moving particles are increased. The obtained results show that the GHZ-state is the most robust state comparing to the others, where the degradation rate is less than that for the other states particularly in the second Rindler region. Also, it is shown here that the entangled property doesn't change in the accelerated frames. Additionally, the paper shows that the degree of entanglement decreases as the accelerations of the particles increase in the first Rindler region. However in the second region, where all subsystems are disconnected at zero acceleration, entangled states are generated as the acceleration increases.

*Keywords*: Multi-qubit states, Non-inertial frame, Fidelity, Capacity, Entanglement, GHZ state, GHZ-like state, W-state.
*Communicated by*: I Cirac & B Terhal

## 1 Introduction

Recently, quantum information theory in the relativistic framework has attracted considerable attention. It seems to be mainly due to the fact that many modern experiments on quantum information processing involve the use of photons and/or electrons, where the relativistic effect is not negligible [1]. The dynamics of entanglement and its applications for traveling systems in non-inertial frames have been investigated by many authors. For example, Alsing et al. (2003) used the accelerated channel to perform quantum teleportation [2]. Landulf et al. (2009) discussed the phenomena of entanglement sudden death and information lose for a two qubits system in the non-inertial frames [3]. Khan et al. (2011) investigated the relativistic quantum game in the non-inertial frames, where the impact of the Unruh effect

on the non-zero sum games was discussed [4]. The dynamics of of a GHZ state in non inertial frame is investiagted by A. Smith et.al (2011), where it is assumed that only one particle is accelerated [5]. However, they investigated the possibility that the accelerated state can't violates Bell and CHSH inequalities for larger acceleration. Metwally (2012) discussed the usefulness of the travelling channels in the non-inertial frames to perform effective quantum teleportation of accelerated and non accelerated information [6, 7, 8, 9]

Futhermore, the dynamics of tripartite qubits in the non-inertial frames have been discussed by many authors from different point of views. For example, Hwang et al. (2001) examined the tripartite entanglement when one of the three parties moves with a uniform acceleration with respect to the other parties [10]. Esfahani et al. (2012) discussed the dynamics of entanglement for three spin $\frac{1}{2}$ massive particles by Gaussian momentum distribution [11].

In this paper, we investigate the behavior of the tripartite entanglement in the non-inertial frames through the GHZ state, GHZ-like state and W-state, where these states could be used to perform many tasks of quantum information. Also, we investigate the fidelity property and the channel capacity property of these three states in the accelerated frames.

The outline of this paper is as follows: An analytical solution for the proposed model for the different three states is introduced in Sec.2. The behavior of fidelities and capacities of the accelerated channels are described in Sec.3. Quantifying the degree of entanglement of the accelerated entangled states is provided in Sec.4. Finally, Sec.5 concludes this paper.

## 2 The Proposed Model

In this section we investigate the behavior of the three different types of multi-qubit states, namely, GHZ, GHZ-like and W-states in the non-inertial frames. These tripartite states have been classified by Dür et al. [12] such that they can't be obtained from each other by using local operation and classical communication. These states have been widely used as quantum channels to perform different quantum information and quantum computations tasks. For example, Karlesson et al. [13] showed that the GHZ state can be utilized to establish teleportation. Due to the new technology, the GHZ state is used as quantum channel to teleport quantum correlation by means of what is called entanglement swapping [14].

Assume that we have three users Alice, Bob and Charlil share one of a pure state in the form:

$$\begin{aligned} |\psi_w\rangle &= \frac{1}{\sqrt{3}}(|001\rangle + |010\rangle + |100\rangle), \\ |\psi_G\rangle &= \frac{1}{\sqrt{2}}(|000\rangle + |111\rangle), \\ |\psi_{GL}\rangle &= \frac{1}{2}(|001\rangle + |010\rangle + |100\rangle + |111\rangle), \end{aligned} \tag{1}$$

where $|\psi_w\rangle, |\psi_G\rangle$ and $|\psi_{GL}\rangle$ represent the W, GHZ and GHZ-like states respectively. It is assumed that these states represent three qubits state of fermions particle of mass $m$ moves in the Mikowski space. It is important to point out that the GHZ state can be prepared from two Bell states shared between the parties. However if one users applies a CNOT and measures the target qubits in the basis "0" or "1" the state terns into a GHZ-like state [15, 16]. On the other hand the tripartite entanglement criterion obeying the local particle-

number superselection rule, where it can be obtained by extending the operational definition of bipartite entanglement of identical particles See ([17] for more details).

Let us consider that these states represent a solution for Dirac equation:

$$i\gamma^{\kappa}(\partial_{\kappa} - \Gamma_{\kappa})\psi + m\psi = 0, \tag{2}$$

where $\gamma^{\kappa}$ represents the Dirac matrices, $\Gamma_{\kappa}$ are spinorial affine connections and $\psi$ is a spinor wave functions [18, 19]. Eq. (3) implies that the physical information formed initially in region I is leaked to the inaccessible region (region II) due to accelerating motion. This loss of information causes a particle detector in the region I to detect a thermally average state, which is a main scenario of Unruh effect [20]. The transformations from Minkowski space to Rindler space are given by:

$$\big|0_k\big\rangle_M = \cos r\big|0_k^+\big\rangle_I\big|0_k^-\big\rangle_{II} + e^{-i\phi}\sin r\big|1_k^+\big\rangle_I\big|1_k^-\big\rangle_{II}, \quad \big|1_k\big\rangle_M = \big|1_k^+\big\rangle_I\big|0_k^-\big\rangle_{II}, \tag{3}$$

where $k = 1, 2$ and 3 for Alice,Bob and Charli respectively. The definition of $r$ is given by $\tan r_k = Exp[-\pi\omega_k c/a_k]$, where $0 \leq r_k \leq \pi/4$, $a_k$ is the acceleration such that $0 \leq a_k \leq \infty$, $\omega_k$ is the frequency of the traveling qubit and $c$ is the speed of light. These transformations divide Rindler space into two regions $I$ and $II$ for fermions and anti-fermions states respectively, (for more details see [21, 6]).

### *2.1 W-state*

The state vector of the W-state is given by $\big|\psi_w\big\rangle$ from Eq. (1). Using the transformation in Eq. (3), we get the W-state vector in both of Rindler regions $I$ and $II$. By calculating the density operator for the W-state and trace out the anti-fermions particles in the second region $II$, we get the accelerated channel of the initial W- state, $\rho_w$ in the first region $I$ as:

$$\begin{aligned}
\rho_W^{(I)} \;=\; & \frac{1}{3}\Big\{\big|100\big\rangle\Big(C_2^2C_3^2\big\langle 100\big| + C_2C_1C_3^2\big\langle 010\big| + C_3C_1C_2^2\big\langle 001\big|\Big) \\
& +\big|010\big\rangle\Big(C_1C_2C_3^2\big\langle 100\big| + C_1^2C_3^2\big\langle 010\big| + C_3C_2C_1^2\big\langle 001\big|\Big) \\
& +\big|001\big\rangle\Big(C_1C_3C_2^2\big\langle 100\big| + C_2C_3C_1^2\big\langle 010\big| + C_1^2C_2^2\big\langle 001\big|\Big) \\
& +\big|101\big\rangle\Big(\big\{S_1^2C_2^2 + C_2^2S_3^2\big\}\big\langle 101\big| + C_2C_1S_3^2\big\langle 011\big| + C_2C_3S_1^2\big\langle 110\big|\Big) \\
& +\big|110\big\rangle\Big(\big\{S_2^2C_3^2 + S_1^2C_3^2\big\}\big\langle 110\big| + C_3C_1S_2^2\big\langle 011\big| + C_3C_2S_1^2\big\langle 101\big|\Big) \\
& +\big|011\big\rangle\Big(\big\{C_1^2S_3^2 + C_1^2S_1^2\big\}\big\langle 011\big| + C_1C_2S_3^2\big\langle 101\big| + C_1C_3S_2^2\big\langle 110\big|\Big) \\
& +\big|111\big\rangle\Big(S_2^2S_3^2 + S_1^2S_3^2 + S_1^2S_2^2\Big)\big\langle 111\big|\Big\},
\end{aligned} \tag{4}$$

where $C_k = \cos r_k$, $S_k = \sin r_k$ and $k = 1, 2, 3$. Similarly if we trace the fermions particles in the first region, $I$, we obtain the state of anti-fermions in the second region $II$ as:

$$\begin{aligned}
\rho_W^{(II)} \;=\; & \frac{1}{3}\Big\{\big|000\big\rangle\Big(C_2^2C_3^2 + C_1^2C_3^2 + C_1^2C_2^2\big\langle 000\big|\Big) \\
& +\big|010\big\rangle\Big(\big\{S_2^2C_3^2 + S_2^2C_1^2\big\}\big\langle 010\big| + S_2S_1C_3^2\big\langle 100\big| + S_2S_3C_1^2\big\langle 001\big|\Big) \\
& +\big|001\big\rangle\Big(\big\{C_1^2S_3^2 + C_2^2S_3^2\big\}\big\langle 001\big| + S_3S_1C_2^2\big\langle 100\big| + S_3S_2C_1^2\big\langle 010\big|\Big)
\end{aligned}$$

$$
\begin{aligned}
&+|101\rangle\Big(S_1^2S_3^2\langle 101| + S_1S_2S_3^2\langle 011| + S_3S_2S_1^2\langle 110|\Big)\\
&+|100\rangle\Big(\{S_1^2C_3^2 + S_1^2C_2^2\}\langle 100| + S_1S_2C_3^2\langle 010| + S_1S_3C_2^2\langle 001|\Big)\\
&+|110\rangle\Big(S_1^2S_2^2\langle 110| + S_1S_3S_2^2\langle 011| + S_2S_3S_1^2\langle 101|\Big)\\
&+|011\rangle\Big(S_2^2S_3^2\langle 011| + S_2S_1S_3^2\langle 101| + S_3S_1S_2^2\langle 110|\Big)\Big\}. \qquad (5)
\end{aligned}
$$

### 2.2 GHZ-state

In the GHZ-state, we assume three users share a three qubits state of GHZ type. In the Rindler space and tracing out the states in the second regions, we get the behavior of $\rho_G$ in the first region as:

$$
\begin{aligned}
\rho_G^{(I)} \;=\;& \frac{1}{2}\Big\{C_3^2\{C_1^2(C_2^2|000\rangle\langle 000| + S_2^2|010\rangle\langle 010|) + S_1^2(C_2^2|100\rangle\langle 100| + S_2^2|110\rangle\langle 110|)\}\\
&+S_3^2\{C_1^2\big(C_2^2|001\rangle\langle 001| + S_2^2|011\rangle\langle 011|\big) + S_1^2\big(C_2^2|101\rangle\langle 101| + S_2^2|111\rangle\langle 111|\big)\}\\
&+C_1C_2C_3\big(|000\rangle\langle 111| + |111\rangle\langle 000|\big)+|111\rangle\langle 111|\Big\}. \qquad (6)
\end{aligned}
$$

To find the density operator $\rho_G$ in the second region $II$, we trace out all the modes in the first region $I$. After performing this procedure, we get the density operator$\rho_G^{(II)}$ which is the same as $\rho_G^{(I)}$ except the last three terms change into $S_1S_2S_3\big(|000\rangle\langle 111| + |111\rangle\langle 000|\big)+|000\rangle\langle 000|$.

### 2.3 GHZ-like state

The GHZ-like state represents another version of the GHZ state, where it can be constructed either from an EPR pair and a single photon or from the GHZ state [22]. In the non-inertial frames this state is transformed into $\rho_{GL}$ in the first region $I$ as:

$$
\begin{aligned}
\rho_{GL}^{(I)} \;=\;& \frac{1}{4}\Big\{|001\rangle\{C_1^2C_2^2\langle 001| + C_1C_3C_2^2\langle 100| + C_2C_3C_1^2\langle 010| + C_1C_2C_3\langle 111|\}\\
&+|010\rangle\{C_1^2C_3^2\langle 010| + C_3C_2C_1^2\langle 001| + C_3^2C_1C_2\langle 100| + C_1C_3\langle 111|\}\\
&+|100\rangle\{C_2^2C_3^2\langle 100| + C_3C_1C_2^2\langle 001| + C_3^2C_2C_1\langle 010| + C_2C_3\langle 111|\}\\
&+|101\rangle\{(S_1^2C_2^2 + C_2^2S_3^2)\langle 101| + C_2C_3S_1^2\langle 110| + S_3^2C_2C_1\langle 011|\}\\
&+|110\rangle\{(S_2^2C_3^2 + S_1^2C_3^2)\langle 110| + C_3C_1S_2^2\langle 011| + C_3C_2S_1^2\langle 101|\}\\
&+|011\rangle\{(C_1^2S_2^2 + C_1^2S_3^2)\langle 011| + S_3^2C_1C_2\langle 101| + C_1C_3S_2^2\langle 110|\}\\
&+|111\rangle\{(S_1^2S_2^2 + S_1^2S_3^2 + S_2^2S_3^2 + 1)\langle 111| + C_1C_3\langle 010| + C_1C_2\langle 001| + C_2C_3\langle 100|\}\Big\}. \qquad (7)
\end{aligned}
$$

On the other hand, the behavior of $\rho_{GL}$ in the second region is described by:

$$
\begin{aligned}
\rho_{GL}^{(II)} \;=\;& \frac{1}{4}\Big\{|000\rangle(C_1^2C_2^2 + C_1^2C_3^2 + C_2^2C_3^2 + 1)\langle 000| + S_1S_3\langle 101| + S_1S_2\langle 110| + S_2S_3\langle 011|\\
&+|001\rangle\{(C_2^2S_3^2 + C_1^2S_3^2)\langle 001| + S_1S_3C_2^2\langle 100| + S_3S_2C_1^2\langle 010|\}\\
&+|010\rangle\{(S_2^2C_3^2 + C_1^2S_2^2)\langle 010| + S_2S_3C_1^2\langle 001| + S_2S_1C_3^2\langle 100|\}\\
&+|100\rangle\{(S_1^2C_2^2 + S_1^2C_3^2)\langle 100| + S_1S_2C_3^2\langle 010| + S_1S_3C_2^2\langle 001|\}\\
&+|101\rangle\{S_1^2S_3^2\langle 101| + S_1S_3\langle 000| + S_1S_2S_3^2\langle 011| + S_3S_2S_1^2\langle 110|\}
\end{aligned}
$$

$$+|110\rangle\{S_1^2S_2^2\langle 110| + S_1S_2\langle 000| + S_1S_3S_2^2\langle 011| + S_2S_3S_1^2\langle 101|\}$$
$$+|011\rangle\{S_2^2S_3^2\langle 011| + S_2S_3\langle 000| + S_3^2S_2S_1\langle 101| + S_1S_3S_2^2\langle 110|\}\Big\}. \quad (8)$$

By this way, we obtained the density operators of the accelerated tripartite channels in the non- inertial frames. The following section addresses some properties of these channels, namely, fidelities and capacities in both regions.

## 3 Fidelities and Capacities of Accelerated Channels

### *3.1 Fidelity*

Here, we investigate the behavior of the fidelities and the capacities of the accelerated channels in both Rindler's regions.

It is well known that the fidelity measures the closeness of the accelerated channel in a specific region to its initial state [2]. Mathematically, the fidelity $\mathcal{F} = tr\Big\{\rho_{initial}\rho_{final}\Big\}$, where $\rho_{initial}$ is given by the GHZ, GHZ-like state or W-state and $\rho_{final}$ is given by the corresponding form of these states in the regions $I$ or $II$. In this context, the fidelities in the first region are given by:

$$\begin{aligned}
\mathcal{F}_W^{(I)} &= \frac{1}{9}\Big\{(C_1^2C_2^2 + C_1^2C_3^2 + C_2^2C_3^2 + 2C_1C_2C_3^2 + 2C_1C_3C_2^2 + 2C_3C_2C_1^2\Big\},\\
\mathcal{F}_G^{(I)} &= \frac{1}{4}\Big\{1 + C_1^2C_2^2C_3^2 + 2C_1C_2C_3\Big\},\\
\mathcal{F}_{GL}^{(I)} &= \frac{1}{16}\Big\{1 + C_1^2(C_2^2 + C_3^2) + C_2^2C_3^2 + 2C_1(C_2 + C_3) + 2C_2C_3 + 2C_1C_2C_3^2\\
&\quad +2C_1C_3C_2^2 + 2C_2C_3C_1^2 + S_1^2(S_2^2 + S_3^2) + S_2^2S_3^2\Big\}. \quad (9)
\end{aligned}$$

In the second region, the corresponding fidelities are given as:

$$\begin{aligned}
\mathcal{F}_W^{(II)} &= \frac{1}{9}\Big\{S_1^2(C_2^2 + C_3^2) + S_2^2(C_1^2 + C_3^2) + S_3^2(C_1^2 + C_2^2) + 2S_1S_3C_2^2 + 2S_2S_3C_1^2 + 2S_1S_3C_2^2\Big\},\\
\mathcal{F}_G^{(II)} &= \frac{1}{4}\Big\{(1 + C_1^2C_2^2C_3^2 + S_1^2S_2^2S_3^2 + 2S_1S_2S_3\Big\},\\
\mathcal{F}_{GL}^{(II)} &= \frac{1}{16}\Big\{S_1^2(C_2^2 + C_3^2) + S_2^2(C_1^2 + C_3^2) + S_3^2(C_1^2 + C_2^2) + 2S_2S_3C_1^2 + 2S_1S_3C_2^2 + 2S_1S_2C_3^2\Big\}.
\end{aligned} \quad (10)$$

Figure 1 shows the behavior of the fidelities $\mathcal{F}$ for the accelerated channels in Rindler regions. Figure 1a describes the behavior of the three tripartite channels in the first region $I$. Generally, it is clear that the fidelities decrease as the accelerations of the moving particles are increased. The minimum values of these fidelities are approached as $r \to \infty$. These minimum values depend on the type of the accelerated channel. It is easy to notice that the lower bound of the fidelity is larger for the W-state and smaller for the GHZ and GHZ like state. However the GHZ state has a larger fidelity than that shown for the GHZ-like state.

The fidelities of the traveling tripartite states in the second region $II$ ,which are given by Eq. (10), are described in Figure 1b. For the normal GHZ state the initial fidelity $\mathcal{F}_G^{(II)} = 0.5$

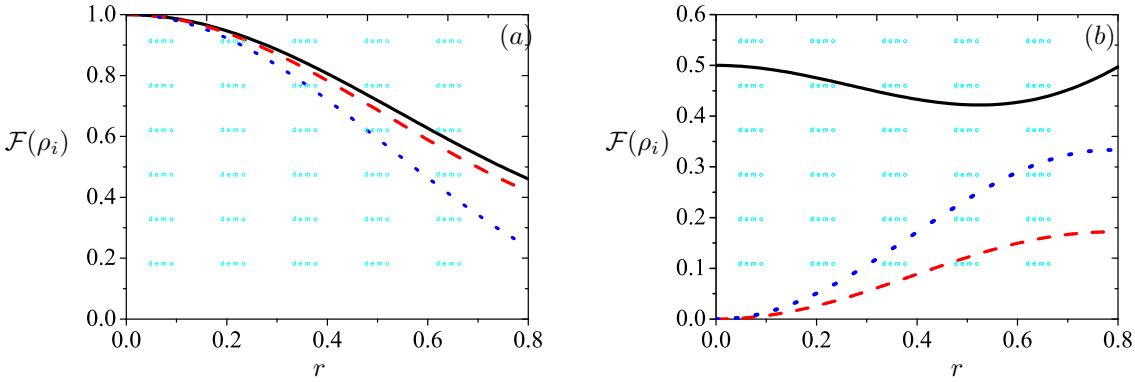


Fig. 1. The fidelities of the accelerated states, where it is assumed that $r_a = r_b = r_c = r$, in (a) the first region and (b) the second region . The solid, dash and dot curves represent $\mathcal{F}(\rho_G^{(i)})$, $\mathcal{F}(\rho_{GL}^{(i)})$ and $\mathcal{F}(\rho_W^{(i)})$ respectively, $i = I$ and $II$. .

at $r_k = 0, k = 1, 2$ and 3. However, as the acceleration increases there will be a small change in its behavior. On the other hand, for the GHZ-like state and the W-state, the fidelities start with zero for zero accelerations. As the accelerations increase, the fidelities $\mathcal{F}_{GL}^{(II)}$ and $\mathcal{F}_W^{(II)}$ increase to reach their maximum values as the accelerations tend to $\infty$. It is clear that the maximum value of $\mathcal{F}_G^{(II)}$ is larger than that depicted for $\mathcal{F}_W^{(II)}$.

### *3.2 Channel Capacity*

All quantum information tasks such as quantum computation and coding information, depend on the capacity of the used quantum channel. Therefore, it is important to evaluate the transmission rate of information from a sender to a receiver. For bipartite state $\rho_{ab}$ the capacity is given by [8]:

$$\mathcal{C}_p = log_a D + \mathcal{S}(\rho_b) - \mathcal{S}(\rho_{ab}), \tag{11}$$

where $\rho_b = tr_a\{\rho_{ab}\}$, $D = 2$ is the dimension of $\rho_a$ and $\mathcal{S}(.)$ is the von Numann entropy. For tripartite particles we introduce the average capacity between each two particles as a measure of the capacity of the accelerated channels. Mathematically, the average capacity is defined as

$$\bar{\mathcal{C}_p}(\rho_{abc}) = \frac{1}{3}\Big(\mathcal{C}(\rho_{ab}) + \mathcal{C}(\rho_{bc}) + \mathcal{C}(\rho_{ac})\Big). \tag{12}$$

Figure 2 shows the behavior of the average capacities of the accelerated channel. Figure 2a describes the dynamics of the average capacities in the first Rindler region $I$, $\bar{\mathcal{C}_p}(\rho_i^{(I)})$, where $i = G, GL$ or $W$ states. As a general behavior the capacities decrease as the accelerations of the particles increase. This means that, the possibility of coding information degrades as the acceleration increases. The diminishing rate is larger for the normal GHZ state and it is smaller for the W-state. However in the second region a similar behavior is depicted in Figure 2b, but the diminishing rate is smaller than that displayed in Figure 2a for each state.

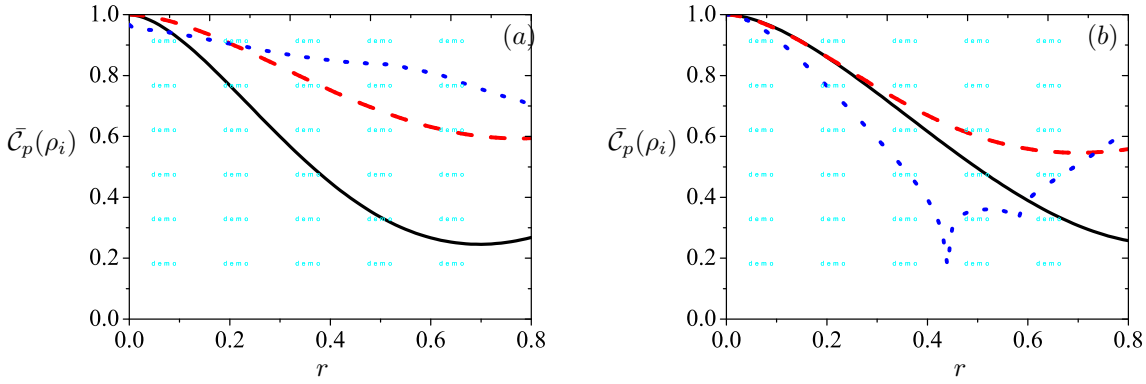


Fig. 2. The average capacities $\bar{\mathcal{C}}_p(\rho)$ of the accelerated channels, where $r_a = r_b = r_c = r$, in (a)the first Rindler Region and (b)the second region. The solid, dash and dot curves represent $\bar{\mathcal{C}}_p(\rho_G^{(i)})$, $\bar{\mathcal{C}}_p(\rho_{GL}^{(i)})$ and $\bar{\mathcal{C}}_p(\rho_W^{(i)})$ respectively, $i = I$ and $II$.

## 4 Entanglement of the Accelerated Entangled States

We proceed now for the most important property that we investigate in this paper. We quantify the degree of entanglement of the travelling states in the Rindler regions. For this aim we use the negativity as a measure of entanglement for three qubit system [23, 24, 25, 26]. The tripartite negativity for the state $\rho_{abc}$ is defined as

$$\mathcal{N}(\rho_{abc}) = \left(\mathcal{N}_{a-bc}\mathcal{N}_{b-ca}\mathcal{N}_{c-ba}\right)^{\frac{1}{3}} \tag{13}$$

where $\mathcal{N}_{i-jk} = 2max\{0, \sum_i |\lambda_i|\}, i = a, b, c$ and $jk = bc, ac, ab$ and $\lambda_i$ are the negative values of the partial transpose of the density operator $\mathcal{N}(\rho_{abc})$.

The entanglement behavior in the first region $I$ of the three tripartite states is described in Figure 3a, where it is assumed that the three particles are equally accelerated. At zero accelerations i.e. $r_1 = r_2 = r_3 = 0$, the entanglement of each state is maximum in the first region $I$, where $\mathcal{N}_G^{(I)} = \mathcal{N}_{GL}^{(I)} = 1$, while for the W-state $\mathcal{N}_W^{(I)} \simeq 0.66$. As the acceleration increases, the entanglement smoothly approachs its minimum values at $r_k \to \infty, k = 1, 2, 3$. It is clear that the degree of entanglement of GHZ-like state is smaller than that shown for the normal GHZ state. The behavior of the W-state is similar than those shown for GHZ family and the $\mathcal{N}(\rho_W)$ is completely vanishes as $r_k \to \infty$.

Figure 3b describes the entanglement of the accelerated entangled states in the second region $II$. It is clear that at zero acceleration, all the accelerated states are separable. As the accelerations $r_k$ increase, the accelerated states turn into entangled states. The degree of entanglement approaches its maximum upper bounds as $r_k \to \infty$.

## 5 Conclusion

In this paper, we investigated some properties of GHZ, GHZ-like state and W-state in the non inertial frames, where it is assumed that all the particles are equally accelerated. Namely, we investigated the fidelities, capacities and entanglement. These phenomena have been

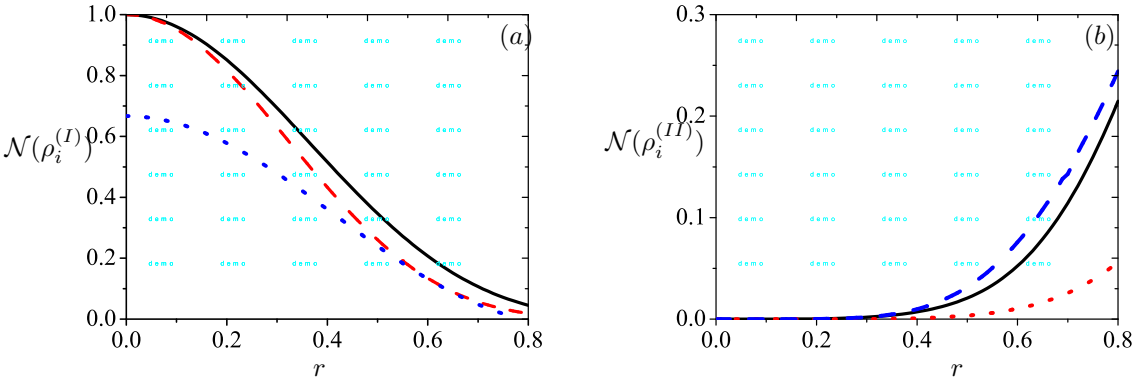


Fig. 3. The entanglement of the accelerated states, where it is assumed that $r_a = r_b = r_c = r$, in (a) the first Rindler region and (b)in the second region. The solid, dash and dot curves represent $\mathcal{N}(\rho_G^{(i)})$, $\mathcal{N}(\rho_{GL}^{(i)})$ and $\mathcal{N}(\rho_W^{(i)})$ respectively, $i = I$ and $II$.

investigated in both Rindler regions. Analytical expressions have been introduced for these quantities for the different accelerated channels.

It is shown here that, the fidelities of the channels in the first Rindler region decrease as the accelerations of the moving particles increase. However the behavior of the fidelities in the second region increase for the GHZ-like state and the W-state, where the fidelities is completely vanish for small values of the accelerations. The upper limit of the fidelity of the GHZ-like state is larger than that depicted for the W-state. On the other hand, for the normal GHZ state the fidelity is fluctuated around 0.5. This asserts that the normal GHZ state is more robust in the second region.

The capacities of the accelerated channels are quantified as the average capacities over all the bipartite subsystems. It is shown that the capacities decrease as the accelerations increase. However For the normal GHZ state the degradation is larger than those depicted for the GHZ-like state and W-state. However the degradation rate in the first Rindler region is larger than that shown in the second Rindler region. Also, for the normal GHZ state the degradation is the biggest one, while it is the smallest for the W-state. This confirmd that, it is possible to code information in the case of W-state better than that for the case of GHZ and GHZ like states.

Quantifying the degree of entanglement of the accelerated entangled states in the different Rindler region are quantified by means of negativity. In the first rindler's region, the entanglement of the generated entangled state decreases as the acceleration of the moving particle increases. However, the decay rate of entanglement for GHZ is smaller than that depicted for GHZ-like state. In the second region, there are entangled states generated for faster accelerations. The upper limit of the degree of entanglement is the biggest for the GHZ state, while for the W-state it is the smallest.

*In conclusion:* the entangled properties of the travelling channels don't change in the non inertial frames. Although the W-state has less degree of entanglement, we can coded more information than through the GHZ and the GHZ-like states. The GHZ state is more robust than GHZ-like state.

**Acknowledgements**

We are grateful to the reviewers for their constructive comments, which helped us to improve the manuscript. Also, we would like to thank Prof. Abdelmageed Aly and Dr. Saleh Aly for their help and support.

**References**

1. M. A. Nielsen and I. L. Chuang (2010), *Quantum computation and quantum information,* Cambridge University Press (Cambridge).
2. P. M. Alsing and G. J. Milburn (2003), *Teleportation with a uniformly accelerated partner,* Phys. Rev. Lett, 91, 180404.
3. A. G. S. Landulfo and G. Matsas (2009), *Sudden death of entanglement and teleportation fidelity loss via the Unruh effect,* Phys. Rev. A, 032315.
4. S. Khan and M. Khan (2011), *Relativistic quantum games in noninertial frames,* J.Phys. A: Math. Theor, 44 355302.
5. A. Smith and R. Mann (2011), *Persistence of tripartite nonlocality for non-inertial observers,* arXiv:1107.4633.
6. N. Metwally (2012), *Usefulness classes of travelling entangled channels in noninertial frames,* arXiv:1201.5941. To appeare in International Journal of Modern Physics B, 2013.
7. N. Metwally (2012), *Teleportation of accelerated information,* J. Opt. Soc. Am. B, Vol.30, No.1, pp. 233-237.
8. N. Metwally (2011), *Quantum dense coding and dynamics of information over Bloch channels,* J. Phys. A :Math. Theor. 44 055305.
9. N. Metwally (2012), *Dynamics of encrypted information in superconducting qubits with the presence of imperfect operations,* J. Opt. Soc. Am. B, Vol.29, pp. 389-396.
10. M. Hwang, D. Park and E. Jung (2001), *Tripartite entanglement in a noninertial frame,* Phys. Rev. A, 83, 012111.
11. B. N. Esfahani and M. Aghaee (2012), *Tripartite entanglements seen from a relativistically moving frame,* Quantum Inf. Processing, Vol.11, pp. 529-540.
12. W. Dür, G. Vidal and J. I. Cirac (2000), *Three qubits can be entangled in two inequivalent ways,* Phys. Rev. A, 62, 062314.
13. A. Karlesson and M. Bourennane (1998), *Quantum teleportation using three-particle entanglement,* Phys. Rev. A, 58, 4394.
14. S. Bose, V. Vedral and P. Knight (1998), *Multiparticle generalization of entanglement swapping,* Phys. Rev. A, 57, 822.
15. Fernando G. S. L. Brandao (2005), *Quantifying entanglement with witness operators*, Phys. Rev. A 72, 022310.
16. S. J. van Enk (2006), *Quantum communication, reference frames, and gauge theory*, Phys. Rev. A 73, 042306.
17. H. M. Wiseman and J. A. Vaccaro (2003),*Entanglement of Indistinguishable Particles Shared between Two Parties* Phys. Rev. Lett. 91, 097902.
18. D. E. Bruschi, J. Louko, E. Martn-Martnez, A. Dragan, and I. Fuentes (2010), *Unruh effect in quantum information beyond the single-mode approximation,* Phys. Rev. A, 82, 042332.
19. E. M.-Martinez, I. Fuentes (2011), *Redistribution of particle and antiparticle entanglement in noninertial frames,* Phys. Rev. A, 83, 052306.
20. W. G. Unruh (1976), *Notes on black-hole evaporation,* Phys. Rev. D 14 670; N. D. Birrel and P. C. W. Davies (1982), *Quantum Fields in Curved Space,* Cambridge University Press (Cambridge, England).
21. P. M. Alsing, I. F. Schuller, R. B. Mann and T. E. Tessier (2006), *Entanglement of Dirac fields in noninertial frames,* Phys. Rev. A, 74, 032326.
22. K. Yang, L. Huang,W.Yang and F. Song (2009), *Quantum teleportation via GHZ-like state,* Int.

J. Theor Phys, Vol.48, pp 516-52.
23. S. Sabin, G. Garca-Alcaine (2008), *A classification of entanglement in three-qubit systems* Phys. J. D 48, 435-442.
24. G. Vidal, R. Werner (2002), *Computable measure of entanglement,* Phys. Rev. A, 65, 032314.
25. Z. Man, Y,-J. Xia and N. Ba An (2008), *Entanglement dynamics for a six-qubit model in cavity QED,* J. Phys. B:At. Mol. Opt. Phys, 41, 155501.
26. N. Metwally (2010), *Information Loss in Local Dissipation Environments,* Int. J. Theor. Phys, Vol.49, pp. 1571.